

ORIGINAL ARTICLE

Synthesis and characterization of stable main-chain polymeric metal complex dyes based on phenothiazine or carbazole units for dye-sensitized solar cells

Xu Chen, Ye Liu, Qiufang Xie, Jun Zhou, Yanlong Liao, Chunxiao Zhu, Tianqi Chen and Chaofan Zhong

Four novel polymeric metal complex dyes (P1–P4) based on phenothiazine or carbazole derivatives, containing complexes of diaminomaleonitrile with Zn(II) or Co(II) were synthesized and characterized by gel permeation chromatography, Fourier transform infrared spectroscopy, UV–visible absorption, cyclic voltammetry and elemental analysis. The dyes based on carbazole derivatives (P3, P4) exhibited wider absorption spectra, and after replacement of the Co(II) coordinated ion with Zn(II), a bathochromic shift in the absorption spectrum was observed. When used in dye-sensitized solar cells (DSSCs), the device sensitized by P3 exhibited the best photocurrent conversion efficiency (2.06%) under standard illumination with a short-circuit photocurrent density (J_{sc}) of 4.54 mA cm⁻², an open-circuit photovoltage (V_{oc}) of 0.67 V and a fill factor (ff) of 67.8%. Moreover, these dyes all exhibited excellent chemical and thermal stability. These results reveal a new path for the design of novel conjugated organic polymer dyes for highly efficient DSSCs.

Polymer Journal (2016) 48, 813–819; doi:10.1038/pj.2016.29; published online 23 March 2016

INTRODUCTION

Dye-sensitized solar cells (DSSCs) have been considered to be feasible alternatives to silicon-based photovoltaic cells because of their ease of fabrication, low cost, and high power conversion efficiency (PCE).^{1,2} Typical DSSCs consist of a nanocrystalline titanium oxide (TiO₂) mesoporous film,^{3,4} a sensitizing dye,^{5,6} an electrolyte containing a redox couple^{7–9} and a platinum-coated counter electrode.^{10,11} One of the most important components in DSSCs is the sensitizer, which can absorb sunlight and inject excited electrons into the conduction band of TiO₂. The power conversion efficiencies of DSSC devices made of ruthenium(II)-based dyes in conjunction with iodide-based electrolytes have achieved a certified solar-to-electric PCE of 11.9 ± 0.4% under full sun illumination (AM 1.5 G, 1000 W m⁻²) after fine structural tuning.^{12–14} These levels have been achieved despite the tricky purification process, toxicity and high cost of ruthenium, which have hampered their wider practical adoption, whereas the PCE of DSSCs based on environmentally friendly porphyrin sensitizers exceeded 13% in 2014,¹⁵ even though their synthesis remains complicated. Moreover, metal-free organic compounds have also demonstrated significant PCEs when applied in DSSCs, but preserving the stability of devices made from these complexes remains a notable challenge. Therefore, a clear need in the further advancement of DSSCs is the development of alternative sensitizers based on stable and inexpensive materials.

Polymers containing transition metal complexes are an exciting and promising class of modern materials. These macromolecules are hybrids of π -conjugated organics and transition metal-containing

polymers. Conjugated organic polymers, such as polyacetylene, polyphenylene, polythiophene, polypyrrole and derivatives of these materials, have been extensively explored.^{16,17} Introducing transition metal ions into π -conjugated polymers has provided enormous opportunities to tune the physical properties of the resulting materials. Unique photophysical, photochemical and electrochemical properties are expected to improve because the interaction between transition metal complexes and conducting polymer backbones is strong, which may lead to a wide range of intriguing physical properties, such as photorefractive effects, photoconductivity and novel redox properties.

Polymeric metal complexes have been investigated for decades¹⁸ but have rarely been applied in light harvesting. The use of these hybrid materials as dye sensitizers in DSSCs is of increasing interest, partly due to their good solubility and strong absorption onto the surface of TiO₂. We sought to exploit the rich photochemical and photophysical phenomena of these metal-containing conjugated polymers to harvest light and expand the applications of DSSCs. In hybrid polymer dyes, the D- π -A structure is a common motif because of its intramolecular charge-transfer characteristics.^{19,20} Taking into account these features of an ideal system, we designed monomers in which the metal was pre-complexed and then conjugated with the reactive core, such that they still were able to undergo polymerization. Many of these systems have been derived from electron-rich thiophene-based monomers, which, when polymerized, afford electroactive materials with novel electronic properties.²¹ In this paper, four novel polymeric metal complex dyes with a carbazole or phenothiazine derivative as an

Key Laboratory of Environmentally Friendly Chemistry and Applications of Ministry of Education, College of Chemistry, Xiangtan University, Hunan, PR China

Correspondence: Professor C Zhong, Key Laboratory of Environmentally Friendly Chemistry and Applications of Ministry of Education, College of Chemistry, Xiangtan University, Yanggutang street, Yuhu district, Xiangtan, Hunan 411105, China.

E-mail: zhongcf798@aliyun.com

Received 5 November 2015; revised 27 December 2015; accepted 5 January 2016; published online 23 March 2016

electron donor, a 2-amino-3-((E)-(5-bromo-3-methylthiophen-2-yl)methyleneamino) maleonitrile (2) metal complex as an electron acceptor and an anchoring group connected with a C=C bond as a π -conjugated system were synthesized through simple, low-cost synthetic procedures. The photophysical and thermal properties of the four polymeric metal complexes were studied, and the performance of DSSCs using these four dyes as photosensitizers was investigated in detail.

EXPERIMENTAL PROCEDURE

Materials

All starting materials were obtained from Shanghai Chemical Reagent Co. Ltd (Shanghai, China) and used without further purification. All solvents used in this work were analytical grade. N,N-dimethylformamide (DMF) and tetrahydrofuran were dried by distillation over CaH_2 .

5-Bromo-3-methylthiophene-2-carbaldehyde (1), 10-octyl-3,7-divinyl-10H-phenothiazine (Ar1) and 9-octyl-3,6-divinyl-9H-carbazole (Ar2) were synthesized according to previously published methodologies.^{22–25} The other materials were common commercial grade and used as received. Solvents were purified with conventional methods.

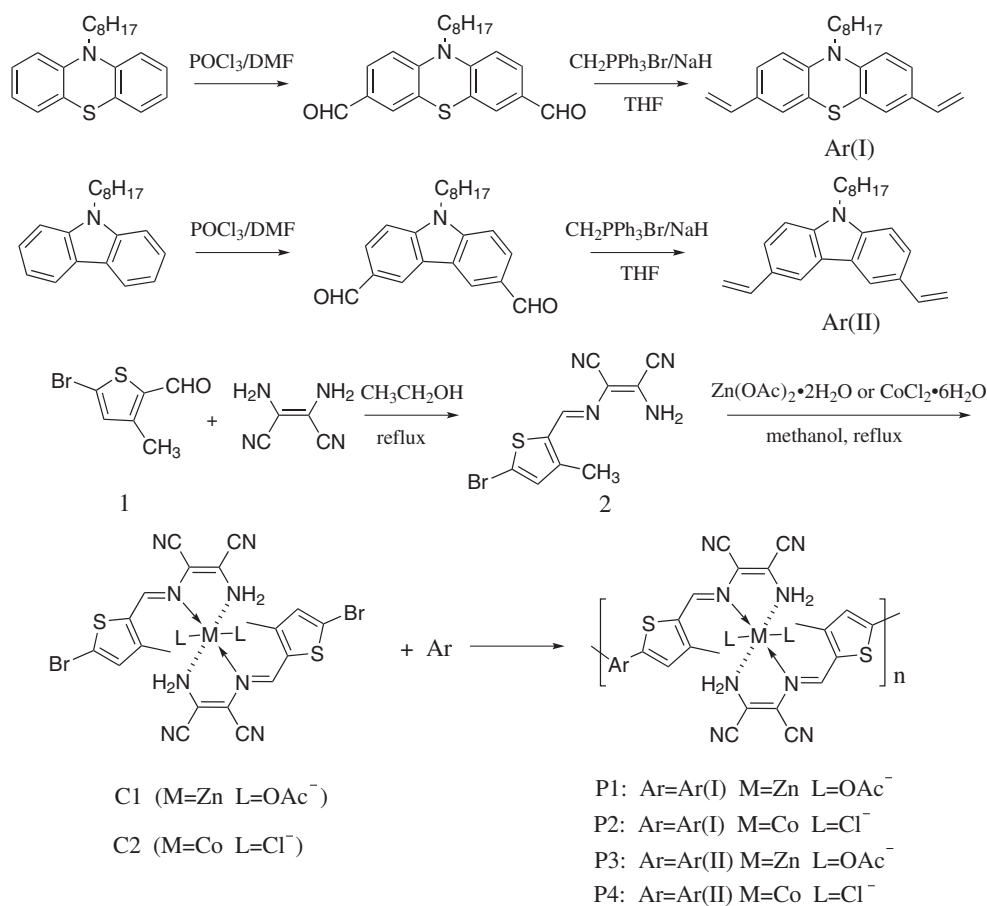
Instruments and measurements

(1) $^1\text{H-NMR}$ spectra were recorded with a Bruker ARX400 (400 MHz) Germany instrument, using tetramethylsilane as an internal standard (0.00 p.p.m.) and DMSO-d_6 or CDCl_3 as the solvent. (2) Fourier transform infrared (FT-IR) spectra were obtained by using KBr pellets. The FT-IR spectrometer range was $450\text{--}4000\text{ cm}^{-1}$. (3) Fluorescence emission spectra (PL) were recorded with a Perkin-Elmer LS-50 model at room temperature with samples prepared in a DMF solution ($10^{-5}\text{ mol l}^{-1}$). (4) UV-visible spectra were

obtained with a PE-Lambda 25 spectrophotometer. Samples were dissolved in DMF and then diluted to a concentration of $10^{-5}\text{--}10^{-4}\text{ mol l}^{-1}$. (5) Thermogravimetric analysis was tested with a Q50 thermal gravimetric analysis instrument manufactured by America in a nitrogen atmosphere at a heating rate of $25\text{ }^\circ\text{C min}^{-1}$ from 25 to $600\text{ }^\circ\text{C}$. (6) Differential scanning calorimetry was tested with a Q10 thermal analyzer at a heating rate of $20\text{ }^\circ\text{C min}^{-1}$ from 25 to $250\text{ }^\circ\text{C}$. (7) Elemental analysis to measure C, H and N of the molecules was performed with an Elementar Vario EL V5 elemental analyzer instrument made by Elementar Analysensysteme (Hanau, Germany). (8) Gel permeation chromatography analyses were performed with Waters Styragel separation columns ($10^3, 10^4, 10^5\text{ \AA}$) and a Waters-1515 model at room temperature, using DMF as the mobile phase and polystyrene as the calibrant. (9) Cyclic voltammetry was performed with a CHI 630C Electrochemical Workstation in a 0.1 mol l^{-1} $[\text{Bu}_4\text{N}]\text{BF}_4$ in DMF solution at a scan rate of 100 mV s^{-1} , using a glassy carbon electrode as the working electrode, a platinum wire electrode as the auxiliary electrode and a saturated calomel electrode as the reference electrode.

Fabrication of DSSCs

Titania paste was prepared as follows: cleaned fluorine-doped SnO_2 conducting glass (FTO) was immersed in a 40 mM TiCl_4 solution at $70\text{ }^\circ\text{C}$ for 30 min, then washed with water and ethanol. The $20\text{--}30\text{ nm TiO}_2$ colloidal particles were coated onto the prepared FTO glass with the sliding glass rod method and were then sintered at $450\text{ }^\circ\text{C}$ for 30 min. This process was repeated two more times to obtain a $15\text{-}\mu\text{m}$ thick TiO_2 film. After cooling to $100\text{ }^\circ\text{C}$, the TiO_2 film was soaked in a 0.5 mM dye-sensitized sample dye in DMF and kept in the dark for 24 h. Then, the films were cleaned by anhydrous ethanol. After drying, electrolyte containing $0.5\text{ mol l}^{-1}\text{ LiI}$, $0.05\text{ mol l}^{-1}\text{ I}_2$ and 0.5 mol l^{-1} 4-tert-butylpyridine was dripped on the surface of the TiO_2 electrodes. A Pt foil used as a counter electrode was clipped onto the top of the TiO_2 as the working electrode. The dye-coated semiconductor film was illuminated through the



Scheme 1 Synthesis of the ligands C1 and C2 and the polymeric metal complexes P1–P4.

conducting glass supported without a mask. The photoelectrochemical performance of the solar cell was measured using a Keithley 2602 SourceMeter (Keithley, Cleveland, OH, USA) controlled by a computer. The cell parameters were obtained under an incident light with intensity of 100 mW cm^{-2} , which was generated by a 500 W Xe lamp passing through an AM 1.5 G filter with an effective area of 0.2 cm^2 .

Synthesis

The synthetic route of all ligands, metal complexes and polymeric metal complexes is shown in Scheme 1.

Synthesis of 2-amino-3-((E)-(5-bromo-3-methylthiophen-2-yl)methyleneamino)maleonitrile (2)

An ethanol solution (100 ml) containing 5-bromo-3-methyl-2-thiophenecarboxaldehyde (1) (2.0326 g, 0.01 mol) was dropped into an ethanol solution (20 ml) containing 2,3-diaminomaleonitrile (1.0810 g, 0.01 mol), and the mixture was refluxed for 16 h. The yellow solution was cooled on ice to yield fine yellow needles, which were filtered off, washed with cooled ethanol, and dried under vacuum (2.2137 g, yield 75%). $^1\text{H-NMR}$ (400 MHz, CDCl_3): 7.62 (s, 1H), 6.74 (s, 1H), 2.35 (s, 1H), 2.21 (s, 1H). Anal. Calcd for $[\text{C}_{10}\text{H}_7\text{BrN}_4\text{S} (2)]$: C, 40.69; H, 2.39; N, 18.98; S, 10.86. Found: C, 41.35; H, 2.24; N, 19.47; S, 11.42. MS: Calcd for $\text{C}_{10}\text{H}_7\text{BrN}_4\text{S} [\text{M}]^+$ 293.96; found, 294.95.

Synthesis of C1

$^{26}\text{Zn}(\text{OAc})_2 \cdot 2\text{H}_2\text{O}$ (0.0549 g, 0.25 mmol) was dissolved in methanol (50 ml) with stirring and refluxing and then added into a methanol (75 ml) solution containing dissolved 2-amino-3-((E)-(5-bromo-3-methylthiophen-2-yl)methyleneamino)maleonitrile (2) (0.1476 g, 0.5 mmol). The mixture was refluxed for 11 h to yield a dark brown precipitate, filtered off, washed with methanol, and dried under vacuum (0.1779 g, yield 92%). Anal. Calcd for $[\text{C}_{24}\text{H}_{20}\text{Br}_2\text{N}_8\text{O}_4\text{S}_2\text{Zn}]$: C, 37.25; H, 2.61; N, 14.48; S, 8.29. Found: C, 36.54; H, 2.42; N, 14.68; S, 8.21. FT-IR (KBr, cm^{-1}): 3457 ($-\text{N}_2\text{H}$), 2237 ($-\text{C}\equiv\text{N}$), 1653 ($\text{C}=\text{C}$), 1582 ($\text{C}=\text{N}$), 1139 ($\text{C}=\text{N-M}$), 945 (Ar-H), 541 (N-M).

Synthesis of C2

$\text{CoCl}_2 \cdot 6\text{H}_2\text{O}$ (0.0594 g, 0.25 mmol) was dissolved in methanol (50 ml) with stirring and refluxing and then added into a methanol (75 ml) solution containing 2-amino-3-((E)-(5-bromo-3-methylthiophen-2-yl)

-methyleneamino)maleonitrile (2) (0.1476 g, 0.5 mmol). The mixture was refluxed for 11 h to yield a dark gray solid, filtered off, washed with methanol, and dried under vacuum (0.1620 g, yield 90%). Anal. Calcd for $[\text{C}_{20}\text{H}_{14}\text{Br}_2\text{Cl}_2\text{N}_8\text{S}_2\text{Co}]$: C, 33.36; H, 1.96; N, 15.56; S, 8.91. Found: C, 33.24; H, 1.85; N, 15.47; S 9.02. FT-IR (KBr, cm^{-1}): 3443 ($-\text{N}_2\text{H}$), 2276 ($-\text{C}\equiv\text{N}$), 1658 ($\text{C}=\text{C}$), 1576 ($\text{C}=\text{N}$), 1127 ($\text{C}=\text{N-M}$), 967 (Ar-H), 550 (N-M).

Synthesis of polymeric metal complex P1

The polymeric metal complex P1 was synthesized by using the Heck coupling method, according to previously described methodology.²⁷ A flask was charged with a mixture of metal complex C1 (0.1145 g, 0.315 mmol), 10-octyl-3,7-divinyl-10H-phenothiazine (0.116 g, 0.315 mmol), $\text{Pd}(\text{OAc})_2$ (0.0024 g, 0.012 mmol), triethylamine (3 ml), tri(o-tolyl)phosphine (0.0220 g, 0.072 mmol) and DMF (8 ml). Then, the flask was vacuum evacuated and purged with N_2 . The mixture was heated at 90°C for 18 h in N_2 . After that, it was filtered after cooling to room temperature, and the filtrate was poured into ethanol. The brown precipitate was filtered and washed with cold ethanol. The crude product was purified by dissolving in DMF and precipitating into ethanol to afford a light brown solid (0.1782 g, yield 58%). FT-IR (KBr, cm^{-1}): 3080 ($\text{C}=\text{C-H}$), 2926, 2854 ($-\text{CH}_2$), 2225 ($-\text{C}\equiv\text{N}$), 1648 ($\text{C}=\text{C}$), 1577 ($\text{C}=\text{N}$), 1124 ($\text{C}=\text{N-M}$), 531 (N-M). Anal. Calcd for $[\text{C}_{48}\text{H}_{47}\text{N}_9\text{O}_4\text{S}_3\text{Zn}]$: C, 59.10; H, 4.86; N, 12.92; S, 9.86. Found: C, 58.89; H, 4.73; N, 12.87; S, 10.02. $M_n = 9.73 \text{ kg mol}^{-1}$, PDI = 1.42.

Synthesis of polymeric metal complex P2

A similar synthetic method as for P1 was used. A flask was charged with a mixture of metal complex C2 (0.2268 g, 0.315 mmol), 10-octyl-3,7-divinyl-10H-phenothiazine (0.1145 g, 0.315 mmol), $\text{Pd}(\text{OAc})_2$ (0.0024 g, 0.012 mmol), triethylamine (3 ml), tri(o-tolyl)phosphine (0.0220 g, 0.072 mmol) and DMF (8 ml), and yielded a gray precipitate (0.1538 g, yield 53%). FT-IR (KBr, cm^{-1}): 3062 ($\text{C}=\text{C-H}$), 2937, 2841 ($-\text{CH}_2$), 2216 ($-\text{C}\equiv\text{N}$), 1644 ($\text{C}=\text{C}$), 1562 ($\text{C}=\text{N}$), 1109 ($\text{C}=\text{N-M}$), 537 (N-M). Anal. Calcd for $[\text{C}_{44}\text{H}_{41}\text{Cl}_2\text{N}_9\text{S}_3\text{Co}]$: C, 57.34; H, 4.48; N, 13.68; S, 10.44. Found: C, 57.21; H, 4.37; N, 13.82; S, 10.36. $M_n = 7.35 \text{ kg mol}^{-1}$, PDI = 1.38.

Synthesis of polymeric metal complex P3

A similar synthetic method as for P1 was used. A flask was charged with a mixture of metal complex C1 (0.2437 g, 0.315 mmol), 9-octyl-3,6-divinyl-9H

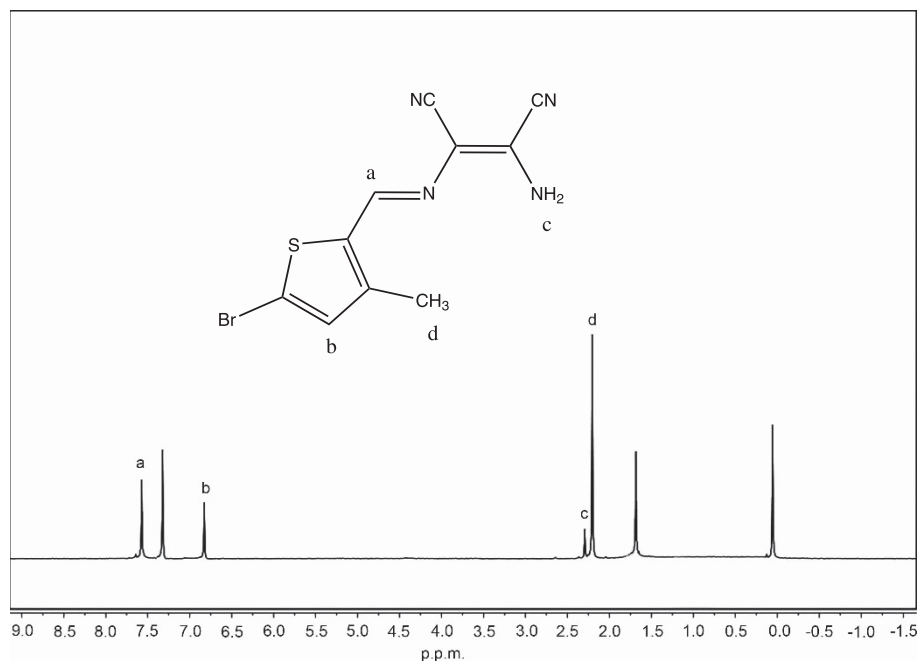


Figure 1 $^1\text{H-NMR}$ spectra of 5-bromo-3-methylthiophene-2-carbaldehyde (1) in CDCl_3 solution.

-carbazole (0.1044 g, 0.315 mmol), Pd(OAc)₂ (0.0024 g, 0.012 mmol), triethylamine (3 ml), tri(*o*-tolyl)phosphine (0.0220 g, 0.072 mmol) and DMF (8 ml), and yielded a yellow solid (0.1485 g, yield 50%). FT-IR (KBr, cm⁻¹): 3029 (C=C-H), 2912, 2845 (-CH₂), 2221(-C≡N), 1643 (C=C), 1572 (C=N), 1119 (C=N-M), 530 (N-M). Anal. Calcd for [C₄₈H₄₇N₉O₄S₂Zn]: C, 61.11; H, 5.02; N, 13.36; S, 6.80. Found: C, 61.04; H, 4.88; N, 13.44; S, 6.71. $M_n = 11.47 \text{ kg mol}^{-1}$, PDI = 1.47.

Synthesis of polymeric metal complex P4

A similar synthetic method as for P1 was used. A flask was charged with a mixture of metal complex C2 (0.2268 g, 0.315 mmol), 9-octyl-3,6-divinyl-9H-carbazole (0.1044 g, 0.315 mmol), Pd(OAc)₂ (0.0024 g, 0.012 mmol), triethylamine (3 ml), tri(*o*-tolyl)phosphine (0.0220 g, 0.072 mmol) and DMF (8 ml) and yielded a pale yellow solid (0.1317 g, yield 47%). FT-IR (KBr, cm⁻¹): 3020 (C=C-H), 2932, 2849 (-CH₂), 2197 (-C≡N), 1625 (C=C), 1557 (C=N), 1101 (C=N-M), 543 (N-M). Anal. Calcd for [C₄₄H₄₁Cl₂N₉S₂Co]: C, 59.41; H, 4.65; N, 14.17; S, 7.21. Found: C, 59.54; H, 4.71; N, 14.28; S, 7.30. $M_n = 8.11 \text{ kg mol}^{-1}$, PDI = 1.37.

RESULTS AND DISCUSSION

Synthesis and characterization

The detailed synthetic routes of the four main-chain polymeric metal complexes (P1–P4) are shown in Scheme 1, and the four polymers (P1–P4) were synthesized via the Heck coupling reaction.²⁸

Figure 1 shows the ¹H-NMR spectrum of the ligand 2-amino-3-((E)-(5-bromo-3-methylthiophen-2-yl)methyleneamino)maleonitrile (2) in which all of its H signals appeared. The IR spectra of the metal complexes C1 and C2 and the polymeric metal complexes P1, P2, P3 and P4 are shown in Figure 2. The broad absorption band appearing at 3500–3280 cm⁻¹ was attributed to the amino group stretching vibration. The peaks of P1, P2, P3 and P4 at 3020–3080 cm⁻¹ corresponded to the stretching vibration of C-H bonds that are adjacent to unsaturated groups. A signal peak appearing at about 2220 cm⁻¹ represented the stretching vibration of the C≡N bond, which became weaker after polymerization. For complexes coordinated with Zn(II), the feature peaks of the C=C bond of P1 and P3 red-shifted to 1648 and 1643 cm⁻¹, respectively, from 1653 cm⁻¹ of C1, and the C=C peaks of Co(II) polymers P2 and P3 also red-shifted to 1644 and 1625 cm⁻¹ relative to C2 at 1658 cm⁻¹ upon the introduction of phenothiazine or carbazole. Analogously, the stretching vibrations of the C=N bond at 1582 and 1576 cm⁻¹ for C1 and C2 red-shifted to 1577, 1562, 1572 and 1557 cm⁻¹ when target polymers (P1–P4), respectively, were formed. The C-N-M stretching vibrations²⁹ of C1 and C2 were at 1139 and 1127 cm⁻¹, and the same peaks of their corresponding target polymers (P1–P4) were red-shifted to 1124, 1119, 1109 and 1101 cm⁻¹. The red-shifts of the unsaturated double bonds above were largely due to the expansion of π -conjugated systems when polymerized. Meanwhile, the N-M stretching vibration peaks of the four polymers were red-shifted to 531, 537, 530 and 543 cm⁻¹ compared with the similar peaks of C1 and C2 that appeared at 541 and 550 cm⁻¹.

The gel permeation chromatography studies showed that the four dyes (P1–P4) had number average molecular weights (M_n) of 9.73, 7.35, 11.47, and 8.11 kg mol⁻¹ with polydispersity index (PDI) values of 1.37–1.47 (Table 1), and the repeating units on average of P1–P4 were 10, 8, 12 and 9, respectively. These results, combined with elemental analysis, indicated that polymerization had taken place between monomers and the target polymeric dyes had been obtained.

Optical properties

The UV-vis absorption of metal complexes C1 and C2 and the polymeric metal complexes (P1–P4) (10⁻⁵ M in DMF solution) are

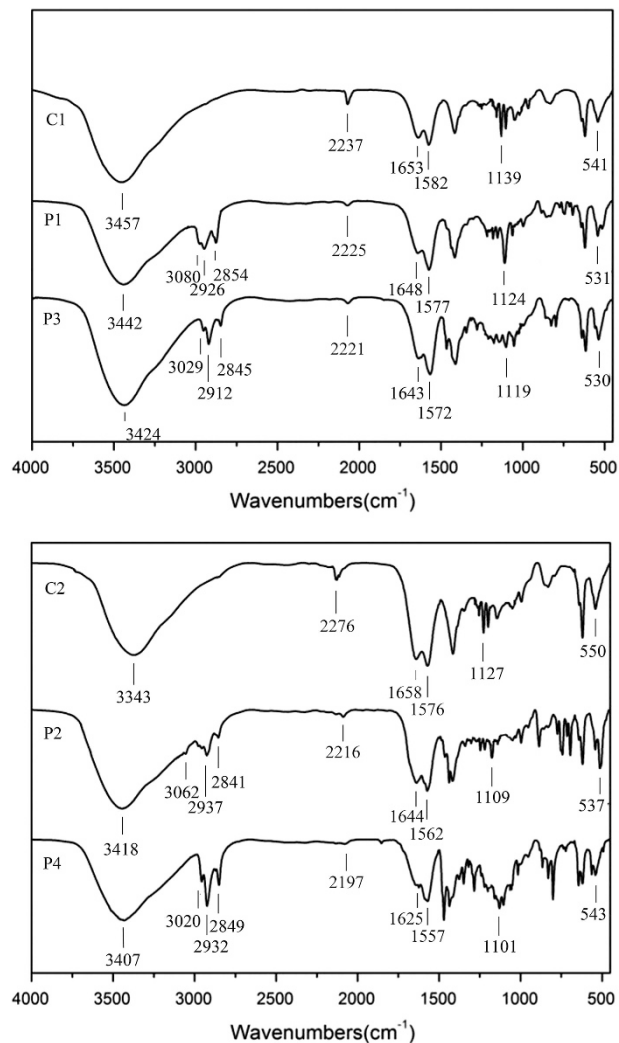


Figure 2 IR spectra of C1, C2, P1, P2, P3 and P4.

shown in Figure 3, and the corresponding data are summarized in Table 2, together with the normalized emission spectral data of the polymeric metal complexes (P1–P4). The light absorption of metal complexes C1 and C2 was primarily attributed to metal-to-ligand charge transfer (MLCT). Compared with the metal complexes C1 and C2, all of the target polymers (P1–P4) had a certain degree of red-shift due to the introduction of the donor units and the increase of π -conjugation in the system after polymerization. The absorption maxima (λ_{max}) of the polymeric metal complexes were in the following order: P3 (438 nm) > P4 (426 nm) > P1 (416 nm) > P2 (405 nm), thus clearly demonstrating that the maximum absorption spectra of the phenothiazine derivative dyes were shorter than those of the carbazole derivative dyes. This phenomenon was probably due to the stronger electron-donating ability of the 9-octyl-3,6-divinyl-9H-carbazole group than that of the 10-octyl-3,7-divinyl-10H-phenothiazine donor. Moreover, we can also observe that zinc(II) metal complexes exhibited longer absorption bands than cobalt(II) metal complexes when polymerized with the same donor, which resulted in increased light harvesting efficiency and higher photogenerated current.

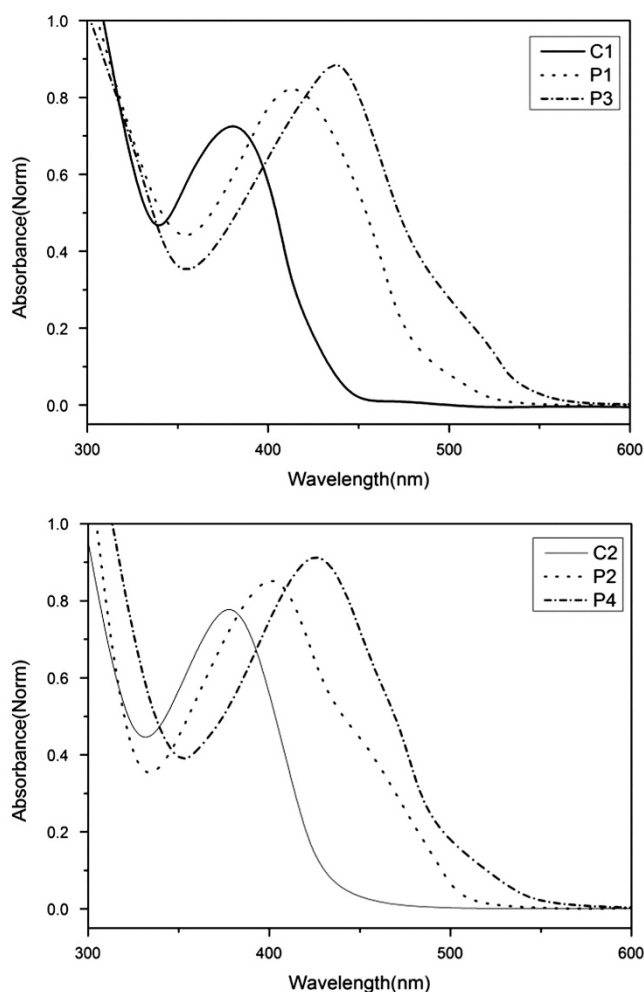
Table 1 Molecular weights and thermal stable properties of the polymeric metal complexes

	Mn^a ($\times 10^3$)	Mw^a ($\times 10^3$)	\bar{X}_n^b	PDI	T_g^c ($^{\circ}C$)	T_d^d ($^{\circ}C$)
P1	9.73	13.8	10	1.42	162	327
P2	7.35	10.14	8	1.38	147	298
P3	11.47	16.86	12	1.47	155	345
P4	8.11	11.12	9	1.37	130	312

^aDetermined by gel permeation chromatography using polystyrene as standard.

^bThe average number of repeating units.

^cDetermined by differential scanning calorimetry with a heating rate of $20\text{ }^{\circ}C\text{ min}^{-1}$ under nitrogen.

^dThe temperature at 5% weight loss under nitrogen.

Figure 3 UV-visible absorption spectra of C1, C2 and polymeric metal complexes (P1, P2, P3, P4) in N,N-dimethylformamide (DMF) solution.

Thermal stability

Stability is an important consideration in the design of DSSCs. The thermal properties of the polymeric metal complexes were investigated by differential scanning calorimetry and thermogravimetric analysis, and the corresponding data are shown in Table 1. The thermogravimetric analysis results (Figure 4) showed that the decomposition temperatures (T_d , the temperature at which 5% weight loss under nitrogen occurs) of the four polymeric metal complexes (P1–P4) were at 327, 298, 345 and 312 $^{\circ}C$ in nitrogen, respectively,

indicating that all of them are stable. The differential scanning calorimetry analysis showed that the four polymers exhibited high glass-transition temperatures (T_g : P1: 162 $^{\circ}C$, P2: 147 $^{\circ}C$, P3: 155 $^{\circ}C$, P4: 130 $^{\circ}C$), which means that solar cells based on these dyes may have longer lifetimes.³⁰ Their high glass-transition temperatures indicate that these materials may have favorable application prospects in improving the stability of DSSCs. The target products did not have fixed melting points, which means that all of them possessed an amorphous structure. It might not be conducive to use this type of structure in organic solar cells.³¹

Electrochemical properties

Electrochemical properties are crucial for materials intended for use in solar cells. The electrochemical behaviors of the polymers were investigated by cyclic voltammetry. Figure 5 shows the cyclic voltammetry curves of P1–P4, which were measured in DMF solution, containing $[Bu_4N]BF_4$ as the supporting electrolyte and using a saturated calomel electrode as the reference electrode at a scan rate of 100 mV s^{-1} . The highest occupied molecular orbital and lowest unoccupied molecular orbital energy levels of these polymers are associated with its E_{ox} and E_{red} . When a saturated calomel electrode is used as the reference electrode, the correlation can be expressed by equations described in the literatures.^{32,33}

The corresponding CV data are summarized in Table 2. The lowest unoccupied molecular orbital energy levels (P1: -3.18 eV ; P2: -3.13 eV ; P3: -3.38 eV ; P4: -3.28 eV) were sufficiently above the conduction band edge of TiO_2 ,³⁴ so we deduced that electrons can be transferred effectively from the excited dye to the TiO_2 . The highest occupied molecular orbital energy values of P1–P4 were estimated to be -5.55 , -5.52 , -5.61 , and 5.57 eV vs saturated calomel electrode, which are lower than the standard potential of the I_3^-/I^- redox couple (4.83 eV vs vacuum), indicating that sufficient driving forces for the regeneration of the oxidized dyes are available. The E_g values of P1–P4 occurred in the following order: P2 (2.39 eV) > P1 (2.37 eV) > P4 (2.29 eV) > P3 (2.23 eV). The phenothiazine (Ar1) electron donor caused a broader lowest unoccupied molecular orbital/highest occupied molecular orbital energy gap than carbazole (Ar2), which indicates that the stronger electron-donating ability of 9-octyl-3,6-divinyl-9H-carbazole units decreased the energy gap.

Photovoltaic properties

The current density–voltage (J – V) curves of the DSSCs based on the four polymer dyes under simulated one-sun illumination (AM 1.5 G, 100 mW cm^{-2}) are shown in Figure 6, and the corresponding parameters of the devices and other relevant data are summarized in Table 3.

The V_{oc} values of the P1–P4 dyes followed the order: P3 > P4 > P1 > P2, which is related to their highest occupied molecular orbital levels. The J_{sc} values of these polymers were very low (P1, $J_{sc} = 4.30\text{ mA cm}^{-2}$; P2, $J_{sc} = 4.21\text{ mA cm}^{-2}$; P3, $J_{sc} = 4.54\text{ mA cm}^{-2}$; P4, $J_{sc} = 4.31\text{ mA cm}^{-2}$). Clearly, the J_{sc} of these dyes did not exceed 5 mA cm^{-2} , probably because of their narrow and short absorption ranges that limited the use of long wavelength energy. The dyes containing Zn(II) had larger J_{sc} values than those containing Co(II), which matched with the absorption λ_{max} of the four polymers. The device sensitized by dye P3 exhibited the best efficiency of 2.06% with a short-current density (J_{sc}) of 4.54 mA cm^{-2} , an open-circuit voltage (V_{oc}) of 670 mV and a fill factor (ff) of 67.8%. The other solar cells sensitized by dyes P1, P2 and P3 had efficiencies from 1.70 to 1.88% and displayed an inverse trend relative to the energy gap (E_g) of these dyes, indicating that the reduction of E_g correspondingly

Table 2 Optical and electrochemical properties of the polymeric metal complexes

Metal complex/Polymer	UV-visible absorbent		PL					
	$\lambda_{abs,max}$ (nm) ^c	$\lambda_{abs,onset}$ (nm) ^c	$\lambda_{em,max}$ (nm) ^c	E_{red} (V) ^a	E_{ox} (V) ^a	HOMO (eV)	LUMO (eV)	E_g (eV) ^b
C1	382	451	—	—	—	—	—	—
C2	377	460	—	—	—	—	—	—
P1	416	522	484	-1.22	1.15	-5.55	-3.18	2.37
P2	405	507	495	-1.27	1.12	-5.52	-3.13	2.39
P3	438	565	465	-1.02	1.21	-5.61	-3.38	2.23
P4	426	540	472	-1.12	1.17	-5.57	-3.28	2.29

Abbreviation: PL, photoluminescence excitation.

^aValues determined by cyclic voltammetry.

^bElectrochemical band gap estimated from highest occupied molecular orbital (HOMO) and lowest unoccupied molecular orbital (LUMO).

^c $\lambda_{abs,max}$, the maximum absorption wavelength in N,N-dimethylformamide (DMF) solution; $\lambda_{abs,onset}$, the onset absorption wavelength in DMF solution; $\lambda_{em,max}$, the maximum emission wavelength in DMF solution.

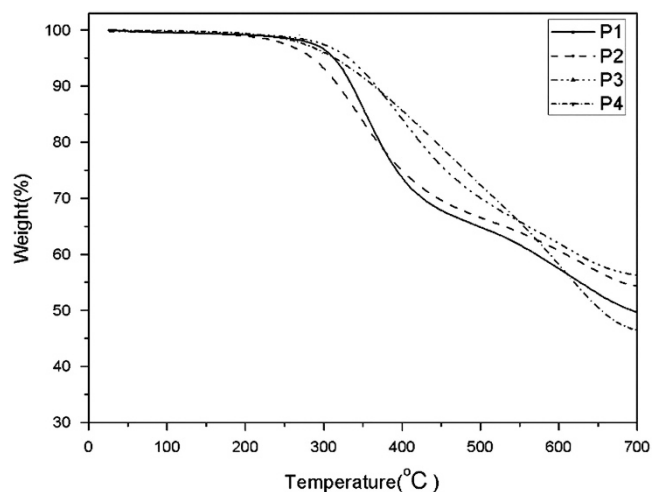


Figure 4 Thermogravimetric analysis curves of P1–P4 with a heating rate of 20 °C min⁻¹ under nitrogen atmosphere.

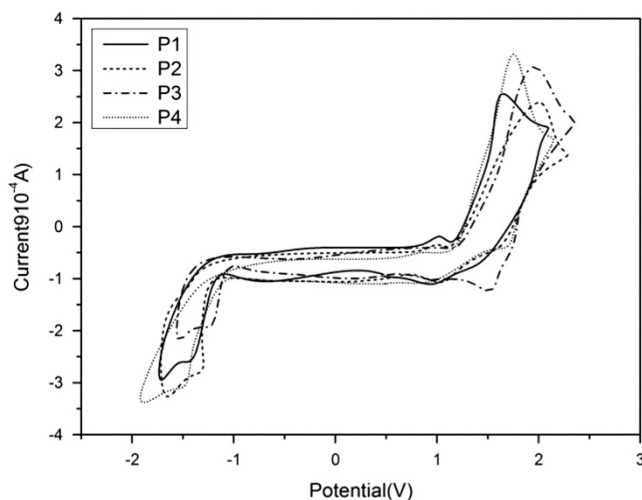


Figure 5 Cyclic voltammograms of P1–P4 in N,N-dimethylformamide (DMF)/0.1 M [Bu₄N]BF₄ at 100 mV s⁻¹.

increases PCEs to some extent. Figure 7 shows the incident photon-to-electron conversion efficiency curves of these four polymeric metal complexes. The maximum external quantum efficiencies (EQE) of

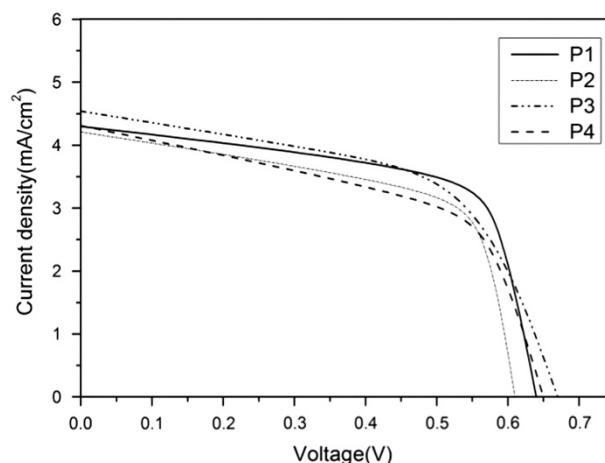


Figure 6 J–V curves of dye-sensitized solar cells based on dyes (P1–P4) under the illumination of AM 1.5, 100 mW cm⁻².

these dyes were very low and no more than 40%, corresponding to the low J_{sc} values.

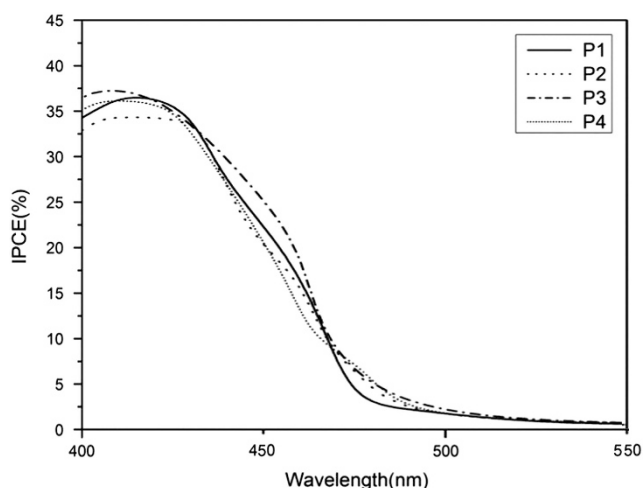
CONCLUSIONS

Four novel dyes (P1–P4) of polymeric metal complexes based on carbazole or phenothiazine derivatives containing complexes of diaminomaleonitrile with Zn(II) and Co(II) were designed, synthesized and applied in DSSCs as sensitizers. These materials exhibited good stability because the metal complex was introduced into the molecular chain. The results showed that different electron-donating groups of the polymer dyes exhibited different photophysical, photovoltaic and electrochemical properties. Incorporation of the 9-octyl-3,6-divinyl-9H-carbazole group into the polymer backbone resulted in more extended electronic delocalization than when the 10-octyl-3,7-divinyl-10H-phenothiazine unit was used, which was reflected in the UV–visible spectra of these dyes. Moreover, the results indicated that the dyes based on d¹⁰ Zn(II) complexes exhibited better performance than dyes based on d⁷ Co(II) complexes on most measured axes, which should aid in the selection of appropriate coordination ions in future work. The power conversion efficiencies of P1–P4 were 1.88, 1.70, 2.06 and 1.82%, respectively. Although the efficiencies are not yet high enough for practical applications, this work reveals a new class of dyes for DSSCs. Because the low PCEs mainly resulted from limited

Table 3 Photovoltaic parameters of devices with sensitizers P1–P4 in DSSCs at full sunlight (AM 1.5 G, 100 mW cm⁻²)

Polymer	Solvent	J_{sc} (mA cm ⁻²)	V_{oc} (V)	ff (%)	η (%)
P1	DMF	4.30	0.64	68.2	1.88
P2	DMF	4.21	0.61	66.1	1.70
P3	DMF	4.54	0.67	67.8	2.06
P4	DMF	4.31	0.65	65.2	1.82

Abbreviations: DMF, N,N-dimethylformamide; DSSC, dye-sensitized solar cell.


Figure 7 Incident photon-to-electron conversion efficiency (IPCE) plots for the dye-sensitized solar cells based on the four polymeric metal complexes (P1–P4) on ITO glass.

J_{sc} values, work is currently in progress to structurally modify these types of dyes to extend their absorption bands and enhance their absorption to obtain higher efficiencies.

CONFLICT OF INTEREST

The authors declare no conflict of interest.

ACKNOWLEDGEMENTS

This work was financially supported by the Open Project Program of the Key Laboratory of Environmentally Friendly Chemistry and Applications of Ministry of Education, China (No.09HJYH10).

- O' Regan, B. & Grätzel, M. A low-cost, high-efficiency solar cell based on dye-sensitized colloidal TiO₂ films. *Nature* **353**, 737–740 (1991).
- Hagfeldt, A., Boschloo, G., Sun, L., Kloo, L. & Pettersson, H. Dye-sensitized solar cells. *Chem. Rev.* **110**, 6595–6663 (2010).
- Chandiran, A. K., Abdi-Jalebi, M., Nazeeruddin, M. & Grätzel, M. Analysis of electron transfer properties of ZnO and TiO₂ Photoanodes for dye-sensitized solar cells. *ACS Nano* **8**, 2261–2268 (2014).
- Zhang, X., Liu, F., Huang, Q. L., Zhou, G. & Wang, Z. S. Dye-sensitized w-doped TiO₂ solar cells with a tunable conduction band and suppress charge recombination. *J. Phys. Chem. C* **115**, 12665–12672 (2011).
- Sauvage, F., Decoppet, J. D., Zhang, M., Zakeeruddin, S. M., Comte, P., Nazeeruddin, M., Wang, P. & Grätzel, M. Effect of Sensitizer Adsorption Temperature on the Performance of Dye-Sensitized Solar Cells. *J. Am. Chem. Soc.* **133**, 9304–9310 (2011).
- Ramkumar, S. & Anandan, S. Synthesis of bianchored metal free organic dyes for dye sensitized solar cells. *Dyes Pigments* **97**, 397–404 (2013).
- Bhargava, R., Daeneke, T., Thompson, S. J., Lloyd, J., Palma, C. A., Reichert, J. & Bach, U. Dual-Function Smart Electrolyte for Dye-Sensitized Solar Cells: 5-Mercaptotetrazoles as Redox Mediator and Corrosion Repressor. *J. Phys. Chem. C* **119**, 19613–19618 (2015).

- Hagfeldt, A. & Grätzel, M. Light-induced redox reactions in nanocrystalline systems. *Chem. Rev.* **95**, 49–68 (1995).
- Jo, Y., Cheon, J. Y., Yu, J., Jeong, H. Y., Han, C. H., Jun, Y. & Joo, S. H. Highly interconnected ordered mesoporous carbon-carbon nanotube nanocomposites: Pt-free, highly efficient, and durable counter electrodes for dye-sensitized solar cells. *Chem. Commun.* **48**, 8057–8059 (2012).
- Thomas, S., Deepak, T. G., Anjusree, G. S., Arun, T. A., Nair, S. V. & Nair, A. S. A review on counter electrode materials in dye-sensitized solar cells. *J. Mater. Chem. A* **2**, 4474–4490 (2014).
- Wu, J., Tang, Z., Huang, Y., Huang, M., Yu, H. & Lin, J. A dye-sensitized solar cell based on platinum nanotube counter electrode with efficiency of 9.05%. *J. Power Sources* **257**, 84–89 (2014).
- Komiya, R., Fukui, A., Murofushi, N., Koide, N., Yamanaka, R. & Katayama, H. Improvement of the conversion efficiency of a monolithic type dye-sensitized solar cell module. Technical Digest, 21st International Photovoltaic Science and Engineering Conference, Fukuoka, Japan, 2C-50-08 (2011).
- Green, M. A., Emery, K., Hishikawa, Y., Warta, W. & Dunlop, E. D. Solar cell efficiency tables (Version 45). *Prog. Photovolt.* **23**, 1–9 (2015).
- Vougioukalakis, G. C., Stergiopoulos, T., Kontos, A. G., Pefkianakis, E. K., Papadopoulos, K. & Falaras, P. Novel Ru (II) sensitizers bearing an unsymmetrical pyridine-quinoline hybrid ligand with extended π -conjugation: synthesis and application in dye-sensitized solar cells. *Dalton Trans.* **42**, 6582–6591 (2013).
- Mathew, S., Yella, A., Gao, P., Humphry-Baker, R., Curchod, B. F., Ashari-Astani, N. & Grätzel, M. Dye-sensitized solar cells with 13% efficiency achieved through the molecular engineering of porphyrin sensitizers. *Nat. Chem.* **6**, 242–247 (2014).
- Bredas, J. L., Silbey, R., Boudreaux, D. S. & Chance, R. R. Chain-length dependence of electronic and electrochemical properties of conjugated systems: polyacetylene, polyphenylene, polythiophene, and polypyrrole. *J. Am. Chem. Soc.* **105**, 6555–6559 (1983).
- Günes, S., Neugebauer, H. & Sariciftci, N. S. Conjugated polymer-based organic solar cells. *Chem. Rev.* **107**, 1324–1338 (2007).
- Lin, C. T., Böttcher, W., Chou, M., Creutz, C. & Sutin, N. Mechanism of the quenching of the emission of substituted polypyridineruthenium (II) complexes by iron (III), chromium (III), and europium (III) ions. *J. Am. Chem. Soc.* **98**, 6536–6544 (1976).
- Ganesan, P., Chandiran, A. K., Gao, P., Rajalingam, R., Grätzel, M. & Nazeeruddin, M. K. Double D- π -A dye linked by 2, 2'-bipyridine dicarboxylic acid: influence of para- and meta- substituted carboxyl anchoring group. *Chem. Phys. Chem.* **16**, 1035–1041 (2015).
- Bryce, M. R. Tetrathiafulvalenes as π -electron donors for intramolecular charge-transfer materials. *Adv. Mater.* **11**, 11–23 (1999).
- Shen, P., Zhao, B., Huang, X., Huang, H. & Tan, S. Synthesis and photovoltaic properties of poly(p-phenylenevinylene) derivatives with two triphenylamine and Bithiophene conjugated side chains. *Eur. Polym. J.* **45**, 2726–2731 (2009).
- Yang, F., Xu, X. L., Gong, Y. H., Qiu, W. W., Sun, Z. R., Zhou, J. W. & Tang, J. Synthesis and nonlinear optical absorption properties of two new conjugated ferrocene-bridge-pyridinium compounds. *Tetrahedron* **63**, 9188–9194 (2007).
- Liu, Y., Li, J., Cao, H., Qu, B., Chen, Z., Gong, Q. & Cao, S. Conjugated polymers containing phenothiazine moieties in the main chain. *Polym. Adv. Technol.* **17**, 468–473 (2006).
- Zhang, X. H., Choi, S. H., Choi, D. & Ahn, K. H. Synthesis and photophysical properties of phenothiazine-labeled conjugated dendrimers. *Tetrahedron Lett.* **46**, 5273–5276 (2005).
- Morin, J. F., Drolet, N., Tao, Y. & Leclerc, M. Syntheses and characterization of electroactive and photoactive 2,7-carbazoleninevinylene-based conjugated oligomers and polymers. *Chem. Mater.* **16**, 4619–4626 (2004).
- Xiao, L., Liu, Y., Xiu, Q., Zhang, L., Guo, L., Zhang, H. & Zhong, C. Novel polymeric metal complexes as dye sensitizers for Dye-sensitized solar cells based on polythiophene containing complexes of 8-hydroxyquinoline with Zn(II), Cu(II) and Eu(III) in the side chain. *Tetrahedron* **66**, 2835–2842 (2010).
- Tsai, L. R. & Chen, Y. Hyperbranched and thermally cross-linkable oligomer from a new 2,5,7-tri-functional fluorene monomer. *J. Polym. Sci. Part A Polym. Chem.* **46**, 70–84 (2008).
- Yu, X., Jin, X., Tang, G., Zhou, J., Zhang, W., Peng, D. & Zhong, C. D- π -A dye sensitizers made of polymeric metal complexes containing 1,10-phenanthroline and alkylfluorene or alkoxybenzene: synthesis, characterization and photovoltaic performance for dye-sensitized solar cells. *Eur. J. Org. Chem.* **26**, 5893–5901 (2013).
- Tajmir-Riahi, H. A. & Theophanides, T. Platinum(II) and magnesium(II) nucleotide complexes. Synthesis, FT-ir spectra, and structural properties. *Can. J. Chem.* **61**, 1813–1822 (1983).
- Tokito, S., Tanaka, H., Noda, K., Okada, A. & Taga, Y. Thermal stability in oligomeric triphenylamine/tris(8-quinolinolato) aluminum electrochromic devices. *Appl. Phys. Lett.* **70**, 1929 (1997).
- Shrotriya, V., Li, G., Yao, Y., Moriarty, T., Emery, K. & Yang, Y. Accurate measurement and characterization of organic solar cells. *Adv. Funct. Mater.* **16**, 2016–2023 (2006).
- Li, X., Zeng, W., Zhang, Y., Hou, Q., Yang, W. & Cao, Y. Synthesis and properties of novel poly(p-phenylenevinylene) copolymers for near-infrared emitting diodes. *J. Eur. Polym. J.* **41**, 2923–2933 (2005).
- Agrawal, A. K. & Jenekhe, S. A. Electrochemical properties and electronic structures of conjugated polyquinolines and polyanthrazolines. *Chem. Mater.* **8**, 579–589 (1996).
- Iqbal, Z., Wu, W. Q., Kuang, D. B., Wang, L., Meier, H. & Cao, D. Phenothiazine-based dyes with bilateral extension of π -conjugation for efficient dye-sensitized solar cells. *Dyes Pigments* **96**, 722–731 (2013).